Functionalized plasmonic lattices for biomolecule detection

Author: Isaac Roca Caritg
Facultat de Física, Universitat de Barcelona (UB), Av. Diagonal 645, 08028 Barcelona, Spain.

Advisor: Xavier Batlle Gelabert

Abstract: Surface-Enhanced RAMAN Scattering (SERS) is the combination of RAMAN scattering and nanoelement surface lattices. By functionalizing Au plasmonic nanoelement arrays with a monolayer of a certain biomolecule, sharp peaks at the SERS spectra can be retrieved. In this report we aim to obtain the RAMAN spectra of 4-mercaptopyridine in an Au lattice of asterisks for two different laser which wavelength is located, respectively,at about a maximum and a minimum of the UV-visible absorption spectra of the lattice.

I. INTRODUCTION

In 1928, C.V. Raman demonstrated that when some radiation is spotlighted to a molecule most of the incident photons are elastically scattered but small portion is inelastically scattered [1] and the difference of the incident and the scattered energy is equal to the vibrational energy associated to some characteristic molecular vibrations [1–3]. However, due to its small cross-section RAMAN scattering is a very weak process [1]. Approximately, only 1 of every 100 photons is inelastically scattered [3].

Several decades later, in 1973, a enhance method was discovered [1, 2] which could increase several orders of magnitude the RAMAN scattering, the so-called Surface-enhanced RAMAN Scattering (SERS). SERS increase the RAMAN scattering by attaching the molecules to study on a plasmonic, nanometre sized, metal lattice [1, 2, 4, 5]. Then, not only matter-light interaction must be considered, but also lattice-light interaction [2]. When the separation of the nanoelements in the lattice is of the order of resonance wavelengths of the latter, every element in the array is excited by the incident light, leading to localized surface plasmonic resonances (LSPR) [4].

The RAMAN scattered signal can be computed as:

$$s_R(\nu_S) = N\sigma^R_{ads}|A(\nu_L|^2|A(\nu_S|^2 I(\nu_L) \tag{1}$$

where S_R is the scattered signal; N the number of particles involved in the SERS; σ^R_{ads} is the increased RAMAN-cross section of the molecule in contact to the nanoelements; and A are the enhance factors for an incident excitation source with intensity $I(\nu_L)$, where ν_L and ν_S refer to the laser and scattered frequencies,respectively [1]. The enhanced factors can be viewed as the ratio of the electric field E resulting from the superposition of the incident field E_{inc} induced by light and the local dipole field induced by the nanoelement, respect to the incident field [1, 2, 5]

$$A(\nu_i) = \frac{E(\nu_i)}{E_{inc}(\nu_i)} \quad where\ i = L, S \tag{2}$$

When the incident frequency is near to the resonance frequency, i.e. the incident and the scattered frequency are similar, the global enhancement factor, at molecule location r_m, can be written as:

$$G_{SERS}(r_m, \nu) = \left| \frac{E(r_m, \nu)}{E_{inc}(\nu} \right|^4 \tag{3}$$

(Equation (3) is discussed in [1, 2, 5])

Areas of the sample where the distance among nanoelements is similar to its resonance wavelengths result in LSPR [1], and this resonant elastic light scattered from the nanoelements yields in an enhancement of local electric field at the molecule location $E(r_m, \nu)$. Thus, if the ratio of $\frac{E}{E_{inc}}$ is 10^2, the total enhancement is $G_{SERS} = \left(10^2\right)^4 = 10^8$. In other words, huge SERS enhancements are conceived from moderate local field E enhancement [2].

The energy lost in the scattering is equal to the vibrational energy of the corresponding mode [1–3], commonly expressed as wave-numbers $\left(cm^{-1}\right)$. It is called RAMAN shift. The expression of the RAMAN shift was deduced from J. Slota et al. [3],

$$RS\left[cm^{-1}\right] = \left(\frac{1}{\lambda_{inc}[nm]} - \frac{1}{\lambda_{sca}[nm]}\right) \times \left(\frac{10^7[nm]}{1[cm]}\right) \tag{4}$$

where λ_{inc} and λ_{sca} are the wavelengths of the incident and the scattered light, respectively.

Due to the enhanced signal, the ease functionalization of metal surfaces and its chemical stability [6], SERS has become the object of multidisciplinary researches, particularly in bioanalytical applications [7]. The aim of this project is to corroborate the usefulness of SERS as a biomolecule detector. Specially this report is focused on the dependence between the signal obtained and the laser used. A wider study could found which nanoelement lattice or which element produce a better enhancement.

To fulfil our goal, we attempted to retrieve the SERS spectra of the 4-mercaptopyridine (4-Mpy) molecule. RAMAN spectrometry facility of the Centres Cientifico-Tecnològics of the University of Barcelona (CCiTUB) were used to capture the SERS spectra. Fourier-transform infra-red spectroscopy (FTIR) was

performed to complement the optical behaviour of the samples at the laboratories of the Institut de Ciència dels MAterials of Barcelona (ICMAB - CSIC).

II. SAMPLES

The samples used in our experiments had a metal-insulator-metal (MIM) configuration (FIG. 1 (a)). Thus, we obtained a broadband response, localized absorption and non-angular dependence [8]. The nanoelement structure consisted on a hexagonal lattice of asterisk-shaped holes, referred to as "star-holes"). A Hexagonal lattice can be viewed as two honeycomb lattices shifted which were proved to have the richest absorption characteristics[8]. Commonly silver and gold are the metals used to produce nanoelement arrays, whereas silver is more plasmonically active, gold has more chemical stability and biocompatibility [1, 2].

The six-bar stars are separated just tens of nanometers allowing a strong near-field coupling within its nearest-neighbours [4, 8]. As the three possible spatial orientations, the array formed by the gaps of faced star-arms can be view as three criss-crossed hexagonal lattices (FIG. 1 (b)) which leads to geometrical frustration when the gaps are excited as localized dipoles [4]. These points, also called hot-spots, are the responsible for the extreme electric field enhancements [2].

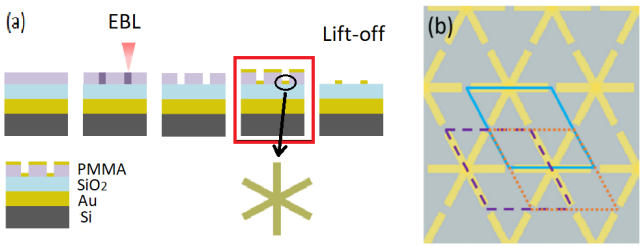

FIG. 1: Scheme of the nanoasterisk array. a) Fabrication of the samples [9]. The sample studied in this TFG did not have the lift-of step b) Top view of the hexagonal lattice with three different spatially oriented criss-crossed sections [4].

To produce the samples, electron beam nanolithography (EBL) and physical vapor deposition [7, 8] are combined for a MIM configuration. First, a layer of 100 nm of Au is deposited upon a silicon substrate by electron beam evaporation (a 5nm Ti layer is used to enhance the adhesion). Then, a layer of SiO_2 is deposited by Plasma Enhanced Chemical Vapor Deposition. To create the nanoelements first a polymethacrylate (950 PMMA A2, MicroChem) is deposited onto the substrate by spin-coating. Later asterisks are defined on the PMMA film by EBL and afterwards, by immersing the sample in two solutions (1:3 MIBK on isopropanol and isopropanol , the methacrylate is removed, and the star-holes performed. Next, Au metallization with electron beam evaporation is realized. Usually, a lift-off procedure is performed as final step i.e., the remaining PMMA is cleared away with acetone and ultrasounds [4, 9], but our sample did not have the lift-off practiced. The result is the one shown in FIG. 1 (a).

The sample fabricated is shown in FIG. 2. We label it with the reference name "S2". It consists of twenty-four enhanced areas distributed in four rows (labelled with numbers) and six columns (labelled with letters), on a Au base surface. The lift-off was not executed. Each row number indicates a different dose factor (DF) used during the EBL, first set up at $180\mu A/cm^2$. By changing this parameter, the width of the stars increases. The letter refers to the hexagonal lattice characteristics. P denotes the *pitch*, which is the distance of two points in phase of the lattice; D the diameter of a circle circumscribed to the star-hole; and W the width of the star-hole bars. These features are summarized in TABLE I

Features (nm)					
Number	DF	Letter	P	D	W
1	1	A	600		45
2	1.2	B	500		45
3	1.4	C	600	450	30
4	1.6	D	500		30
		F	600		20
		G	500		20

TABLE I: Features of the sample used for the SERS. DF is given in multiple of the initial dose factor, $180\mu A/cm^2$; P refers to the pitch, D to the diameter of a circle circumscribed to the star, and W to the designed width of the bars.

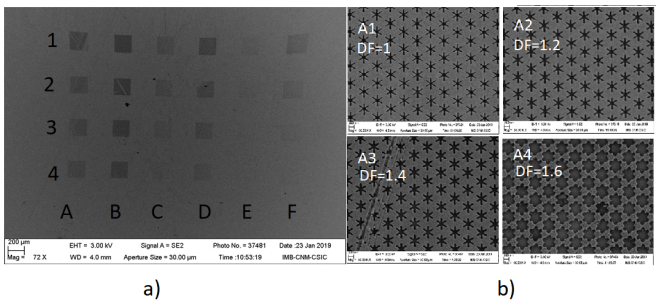

FIG. 2: (a) Sample S2. (b) Magnification of row A, where different widths are appreciated due to an increase of the dose factor, DF.

III. SERS EXPERIMENTAL PROCEDURE

SERS spectra were measured with a Jobin-Yvon LabRam HR 800 dispersive spectrometer couple to an Olympus BXFM optical microscope with an x100 objective. The laser lines are: 532 nm JDSU 20mW (DPSS laser) and 785nm TEC-120-0780-150 (Sacher

Lasertechnik). All spectra were obtained by the mean of five accumulations of five seconds.

Before practising the functionalization i.e., depositing the target molecule –4-mercaptopyridine (4-Mpy)– on the sample, the sample was cleaned with deionized water, argon gas was used to blow the residual water drops, and finally it was dried on the lab heater. Cleaning reduces background noise on the SERS measurement. Eliminating leftover molecules on the surface creates a better environment for the 4-Mpy molecules to bind the Au nonoelements.

The sample is functionalized by deep coating with a 10^{-4} M solution of 4-Mpy (Sigma-Aldrich, 95%). The surface is submerged in a Petri dish with 25 ml of solution, covered with another Petri dish and left resting for a day. 4-Mpy binds to the Au nanoelements via the S caption of the thiol group [6]. This is a strong bond which makes difficult to erase 4-Mpy from the sample once functionalization procedure has taken place. Afterwards, the sample is cleaned again with deionized water to clear the 4-Mpy molecules which hadve not bind to the Au. As 4-Mpy molecules can degrade with heat, we dried the sample in the heater carefully. A 4-Mpy monolayer is obtained this way onto the Au nanoelements [6, 10].

Finally, SERS spectra were measured before and after functionalization to compare the background and to distinguish the peaks of 4-Mpy.

IV. RESULTS AND DISCUSSION

A. FTIR

To understand how our sample respond to light optical characterization in the visible range was performed before and after functionalization. The equipment used was an UV and visible spectrophotometer (Specord 205, Analytic Jena). The absorption spectra of sample S2 show two maxima near a wavelength of $\lambda = 495$nm and $\lambda = 850$nm, and a minimum near $\lambda = 750$nm. The sample exhibits some shift on the maxima after functionalization. However, no general trend was found in the shift.

As presented in TABLE II, when the incident light has $\lambda = 750$, the absorption i.e., the amount energy that interacts with the sample, is very weak. Columns A and B had quite higher absorption, but those areas showed some pollution even after cleaning and its spectre was not useful. Nevertheless, $E1$, $E2$, $E3$ and $F1$ near-zero spectra can be explained from its near-zero absorption coefficient. Comparing TABLE III and IV is seen that the absorption is higher when $\lambda = 495$ than $\lambda = 850$.

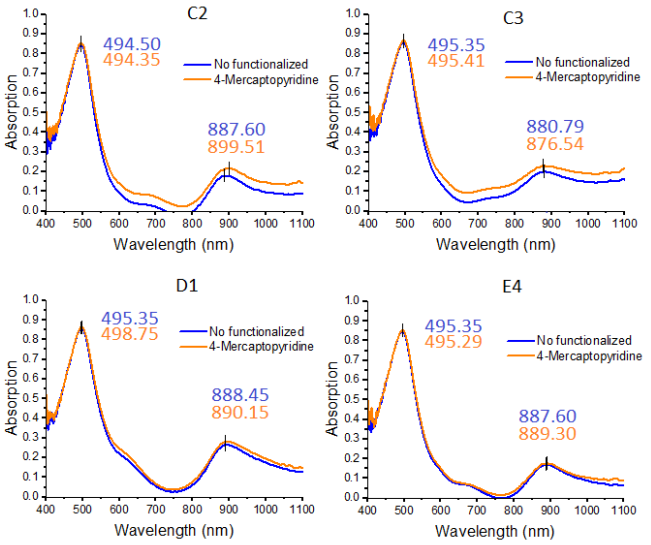

FIG. 3: FTIR measurements for the samples $C2$, $C3$, $D1$ and $E4$. Both maxima are marked. A small shift is observed.

Absorption $\lambda = 750$ nm						
Row number	Column letter					
	A	B	C	D	E	F
1	0.0217	0.0507	0.0741	0.0269	0.0056	0.0341
2	0.1037	0.0863	0.0202	0.1427	0.0408	0.0003
3	0.0661	0.1008	0.0439	0.1407	0.0037	0.0313
4	0.2875	0.1488	0.0661	0.1429	0.0013	0.1727

TABLE II: Values of the absorption coefficient in the minimum. Absorption coefficient is given as a fraction of the impinging light.

Absorption $\lambda = 495$						
Row number	Column letter					
	A	B	C	D	E	F
1	0.8691	0.9037	0.8334	0.8587	0.8519	0.8563
2	0.8714	0.9194	0.8436	0.8822	0.8605	0.8651
3	0.8961	0.8713	0.8605	0.8914	0.8541	0.9119
4	0.8759	0.9421	0.8749	0.9188	0.8509	0.9035

TABLE III: Values of the absorption coefficient in the first maximum. Absorption coefficient is given as a fraction of the impinging light.

B. RAMAN - $\lambda = 785$ nm laser

FIG. 4 show some of the RAMAN spectra, as obtained, without any data treatment.The top right corner inset shows those spectra that had anomalous peaks. As being of the same zone of the sample they are supposed to be caused by some contaminant agent. For a deeper study, a baseline was subtracted to the RAMAN measurements. This way, the resulting spectra only contain the peaks associated to 4-Mpy and its relative

Absorption $\lambda = 850$						
Row number	Column letter					
	A	B	C	D	E	F
1	0.2356	0.2854	0.1824	0.2650	0.2447	0.2673
2	0.3237	0.3154	0.1797	0.2678	0.2757	0.2700
3	0.3491	0.3114	0.2002	0.2920	0.2396	0.2409
4	0.6378	0.3689	0.2632	0.3641	0.1718	0.1873

TABLE IV: Values of the absorption coefficient in the second maximum. Absorption coefficient is given as a fraction of the impinging light.

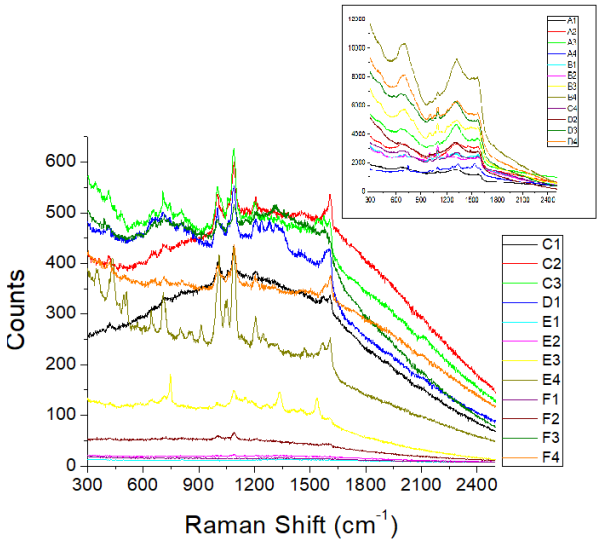

FIG. 4: SERS spectra of S2 with the laser of $\lambda = 785$ nm.

height should be in agreement with the expected ratio for that molecule (FIG: 5). The peaks are reproducible in large part of the sample i.e., show the same RAMAN Shift. 4-Mpy vibrational modes can be characterised by some principal intense peaks [10], while, secondary minor peaks are disguised with the background. Besides, the intensity of the spectra for $E1$, $E2$, $E3$ and $F1$ was close to zero in concordance with its nearly zero absorption factor (TABLE II).

Following Y. Mo et al. [10], the 425 nm peak corresponts to a ring stretch with C-S/C-C-C; the 712 nm, 1061 nm and 1217 nm peaks to a C-H deformation; the 1005 nm peak to an aromatic ring breathing; the 1099 nm peak to a trigonal ring breathing; and the 1581 nm and 1612 nm peaks to a ring stretch with the N.

C. RAMAN - $\lambda = 532$ nm laser

The first absorption peak of FTIR was centred at about $\lambda = 495$ nm, (FIG.3), while the absorption coefficients were close to one (TABLE III), so we decided to continue the study by using a RAMAN laser

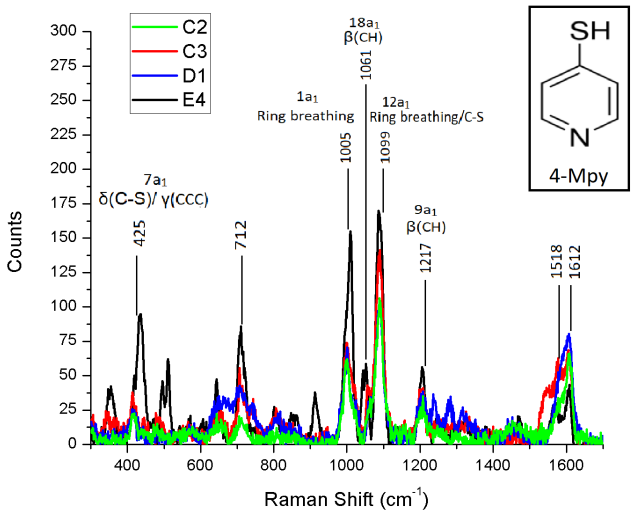

FIG. 5: RAMAN peaks after background substraction for samples $C2$, $C3$, $D1$ and $E4$. The expected peaks of 4-Mpy [10] together with its assignment [6]. are also indicated.

whose wavelength was similar to that value ($\lambda = 532$ nm laser). More clearly enhanced SERS peaks were expected from the new measurement. Unfortunately fluorescence precluded obtaining any quantitative information (FIG. 6).The higher the laser frequency, the higher the fluorescence peaks. Consequently, the 532 nm laser yielded much worse results than the 785 nm one.

Lasers used for SERS have an energy of tenth of eV or even eV. Otherwise, the vibrational modes studied have energies of thousandth of eV. So, on top of the inelastic collision (RAMAN process), molecules can be excited to higher molecular energetic modes absorbing part of the incident light. When deexcitation occurs, radiation with the same energy as the absorbed is emitted. This process is known as fluorescence. In the presence of strong fluorescence signal, RAMAN excited vibrational modes are masked by excited energetic modes of the molecular bond (FIG. 6 (b) and (d)). Furthermore, it cannot be determined whether the fluorescence comes from Au itself, the PMMA leftovers after the lithography process or even 4-Mpy. In the case of PMMA, a lift-off step could solve the problem, but that would reduced the SERS signal itself very much. If fluorescence appears either from Au or 4-Mpy, the signal could be quenched by spotlighting the sample the time enough to make the fluorescence deexcitations occurs and then, make the measurement when the intensity of the fluorescence has decreased. Unfortunately, 4-Mpy degrades when focused with the 532 nm laser making the quenching impossible.

It could be that all the molecules (Au, PMMA, 4-Mpy) flourish due to the impinging of the laser. As it would be a superposition of the fluorescence and we do not have any Au sample measured with that laser before nanoasterisks arrays were created, we cannot determine which molecule was flourishing. Given the amplitude of the fluorescent signal, there is no way to substract it

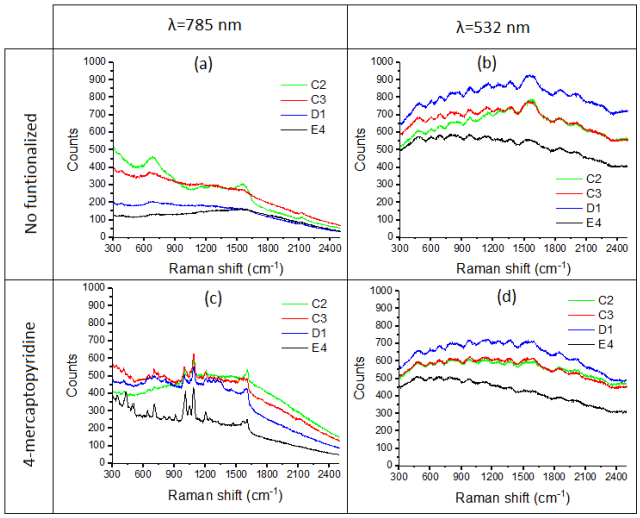

FIG. 6: Comparison of the samples $C2, C3, D1$ and $E4$ on different measurements. Measurements:(a) No functionalized sample with 785 nm laser; (b) No functionalized sample with 532 nm laser; (c) 4-Mpy functionalized sample with 785 nm laser; (d) 4-Mpy functionalized sample with 532 nm laser.

in a quantitative manner. Consequently, it is clear that even the $\lambda = 785$ nm laser yield a less intensive spectra, both the fluorescent signal and the 4-Mpy degradation are much lower than those for the $\lambda = 532$ nm laser.

V. CONCLUSION

To date, we have achieved the goal of finding the principal peaks of the 4-Mpy monolayer with SERS, beginning with a concentration of 10^{-4} M.

We have also proved that the intensity of the peaks is related to the absorption of the light, i.e., to the wavelength of the laser. The laser of $\lambda = 785$ nm falls in a minimum of the absorption spectra. Even so, the peaks found can evidence the presence of 4-Mpy. The laser of $\lambda = 532$ nm falls in a maximum of the absorption spectra, but unfortunately, its energy its high enough to create a fluorescence signal which cannot be quenched without degrading the sample. A laser with a wavelength near to $\lambda = 850$ nm could be the next step. We could take advantage that it falls on the second maximum observed in the FTIR response (FIG. 3), its energy is low enough to avoid unquenchable fluorescence and its absorption coefficient is not very much reduced. Thus, sharpened and more intensive peaks may be recorded using a 850 nm laser.

Comparing the enhancement of the signal with respect to the lift-off performed on the sample, demonstrating the relation between the dose factor in the EBL to the enhanced signal or finding the critical concentration where we could still find 4-Mpy could be the object of further investigation.

Acknowledgements

I would like to thank the Prof. Xavier Batlle for his support, guidance and reliance. Also, all my gratitude to the Ph.D. student Mariona Escoda for tracking my research and for all the knowledge shared without which this article could not be possible. As well, to Tariq Jawhari and Isaac Godoy from CCiTUB and Pau Molet from ICMAB

Finally, I would thank all the support and enthusiasm received from my parents and friends.

[1] G.A. Baker, D.S. Moore, *Progress in plasmonic engineering of surface-enhanced RAMAN-scattering substrates toward ultra-trace analysis*, Anal Bioanal Chem **382**, 1751-1770 (2005)

[2] S. Schücker, *Surface-Enhanced RAMAN Spectroscopy: Conceps and Chemical Application*, Angew. Chem. Int. **53**, 4756-4795 (2014)

[3] I. Gajdoš, F. Greškovic, J. Slota, L'. Dulebová, *Raman Spectroscopy in Polymer Processing Technologies*, Acta Mechanica Slovaca **15**, No. 4, 69-73 (2011)

[4] A. Conde-Rubio, A.Fraile, X. Borrisé, F. Perez-Murano, X. Batlle, A. Labarta, *Geometric frustation in a hexagonal lattice of plasmonic nanoelemetns*, Optics Express **26**, No. 16, 20211-20224 (2018).

[5] K. Kneipp, Y. Wang, H, Kneipp, L.T. Perelman, I. Itzkan, R.R. Dasari, M.S. Feld, *Single Molecule Detection Using Surface-Enhanced RAMAN Scattering (SERS)*, Physical Review Letters **78**, No. 9, 1667-1670 (1997)

[6] J. Hu, B. Zhao, W. Xu, B. Li, Y. Fan, *Surface-enhanced RAMAN spectroscopy study on the structure changes of 4-mercaptopyridine adsorbad on silver substrates and silver colloids*, Spectrochimica Acta Part A **58**, 2827-2834 (2002)

[7] R.Alvarez-Puebla, B. Cui, J.P. Bravo-Vazquez, T. Veres, H. Fenniri, *Nanoimprinted SERS-Active Substrates with Tunable Surface Pasmon Resonance*, J. Phys. Chem. C **111**, 6720-6723 (2007)

[8] A. Conde-Rubio, A.Fraile, A. Espinha, A. Mihi, F. Perez-Murano, X. Batlle, A. Labarta, *Geometric frustation in ordered lattices of plasmonic nanoelemetns*, Scientifics Reports **9**, 3529 (2019).

[9] A. Conde-Rubio, (2018) *Simulations, nanofabrication and optical characterization of plasmonic nanostructures* (Doctoral dissertation). Retrieved from `https://magneticnanomaterialsub.files.wordpress.com/2018/11/tesisacr.pdf`.

[10] L. Zhang, Y. Bai, Z. Shang, Y. Zhang, Y. Mo, *Experimetnal and theoretical studies of RAMAN spectroscopy on 4-mercaptopyridine aqueous solution and 4-mercaptopyridine/Ag complex system*, J. RAMAN Spectrosc. **38**, 1106-1111 (2007)